



香港城市大學
City University of Hong Kong

專業 創新 胸懷全球
Professional · Creative
For The World

CityU Scholars

Efficient rare event simulation for failure problems in random media

LIU, Jingchen; LU, Jianfeng; ZHOU, Xiang

Published in:

SIAM Journal on Scientific Computing

Published: 01/01/2015

Document Version:

Final Published version, also known as Publisher's PDF, Publisher's Final version or Version of Record

Publication record in CityU Scholars:

[Go to record](#)

Published version (DOI):

[10.1137/140965569](https://doi.org/10.1137/140965569)

Publication details:

LIU, J., LU, J., & ZHOU, X. (2015). Efficient rare event simulation for failure problems in random media. *SIAM Journal on Scientific Computing*, 37(2), A609-A624. <https://doi.org/10.1137/140965569>

Citing this paper

Please note that where the full-text provided on CityU Scholars is the Post-print version (also known as Accepted Author Manuscript, Peer-reviewed or Author Final version), it may differ from the Final Published version. When citing, ensure that you check and use the publisher's definitive version for pagination and other details.

General rights

Copyright for the publications made accessible via the CityU Scholars portal is retained by the author(s) and/or other copyright owners and it is a condition of accessing these publications that users recognise and abide by the legal requirements associated with these rights. Users may not further distribute the material or use it for any profit-making activity or commercial gain.

Publisher permission

Permission for previously published items are in accordance with publisher's copyright policies sourced from the SHERPA RoMEO database. Links to full text versions (either Published or Post-print) are only available if corresponding publishers allow open access.

Take down policy

Contact lbscholars@cityu.edu.hk if you believe that this document breaches copyright and provide us with details. We will remove access to the work immediately and investigate your claim.

EFFICIENT RARE EVENT SIMULATION FOR FAILURE PROBLEMS IN RANDOM MEDIA*

JINGCHEN LIU[†], JIANFENG LU[‡], AND XIANG ZHOU[§]

Abstract. In this paper we study rare events associated to the solutions of an elliptic partial differential equation with a spatially varying random coefficient. The random coefficient follows the lognormal distribution, which is determined by a Gaussian process. This model is employed to study the failure problem of elastic materials in random media in which the failure is characterized by the criterion that the strain field exceeds a high threshold. We propose an efficient importance sampling scheme to compute the small failure probability in the high threshold limit. The change of measure in our scheme is parametrized by two density functions. The efficiency of the importance sampling scheme is validated by numerical examples.

Key words. random media, rare event, importance sampling, Gaussian random function

AMS subject classifications. 65C05, 82D30

DOI. 10.1137/140965569

1. Introduction. The study and computation of rare events in stochastic systems have received intensive attention in recent years. Rare events, though they do not occur often, represent the most severe consequence of uncertainty and random effects. The study of these rare events hence gives crucial understanding and has important applications. However, due to the small probabilities of occurrence of such events, quantification casts a serious challenge for conventional probabilistic methods. For example, a direct Monte Carlo strategy to estimate the vanishing small probability will require a huge number of sample points to give estimates with small relative error; in other words, the huge relative variance of these estimators makes them incapable of accurate prediction.

In this work, we aim at developing an efficient important sampling strategy to study the rare events associated with a materials failure problem. The method we develop in this work applies to the general linear elasticity model. For simplicity, we will restrict our discussions here to a scalar model in two dimensions, which can be viewed as a model for out-of-plane deformation of an elastic membrane under external forcing. Similar equations also arise from other contexts, such as groundwater hydraulics and electrostatic response of a planar media. Let $D \subset \mathbb{R}^2$ be an open domain with smooth boundary, which is the equilibrium configuration of the membrane. We consider an out-of-plane displacement field u given by the following boundary

*Submitted to the journal's Methods and Algorithms for Scientific Computing section April 17, 2014; accepted for publication (in revised form) December 17, 2014; published electronically March 3, 2015.

<http://www.siam.org/journals/sisc/37-2/96556.html>

[†]Department of Statistics, Columbia University, New York, NY (jcliu@stat.columbia.edu). This author was supported in part by NSF CMMI-1069064, NSF SES-1323977, and Army grant W911NF-14-1-0020.

[‡]Department of Mathematics, Physics, and Chemistry, Duke University, Durham, NC 27708 (jianfeng@math.duke.edu). This author was supported in part by the Alfred P. Sloan Foundation and NSF grant DMS-1312659.

[§]Department of Mathematics, City University of Hong Kong, Tat Chee Avenue, Hong Kong SAR (xiang.zhou@cityu.edu.hk). This author acknowledges the financial support from a CityU Start-Up grant (7200301) and Hong Kong Early Career Schemes (109113).

value problem:

$$(1.1) \quad \begin{cases} -\nabla \cdot (a(x)\nabla u(x)) = f(x) & \text{for } x \in D; \\ u(x) = 0 & \text{for } x \in \partial D. \end{cases}$$

Here f is the body force acting on the material and $a : D \rightarrow \mathbb{R}$ gives the stiffness of the material. We assume that the membrane is attached to a frame at the boundary ∂D and hence the Dirichlet boundary condition in (1.1) is used here. We assume that the external force f is bounded, that is, there exists a constant $M \in \mathbb{R}$ such that

$$(1.2) \quad |f(x)| \leq M, \quad x \in D.$$

We study the behavior of the material under the influence of internal randomness, which may be a result of manufacture processing or the uncertainty in material properties at the microscopic level. We adopt a probabilistic viewpoint of the complexity and heterogeneity inherent in the material and hence view the stiffness coefficient $a(x)$ as a positive random field. To be more specific, we assume that $a(x)$ is a lognormal random field, that is,

$$(1.3) \quad a(x) = \exp(-\xi(x)), \quad x \in D,$$

where ξ is a stationary Gaussian random field. The lognormal assumption is often used in failure modeling, as it yields good fittings to data (see, for example, [25]). It is also quite natural from the mathematical point of view, as the equation is then almost surely uniformly elliptic. To simplify notation and without loss of generality, we assume that $\mathbb{E}\xi(x) = 0$ and $\text{Var} \xi(x) = 1$. For a general stationary Gaussian random function, our methodology and algorithm have no big difference and we shall elaborate this point in a remark later in section 2.

The random field viewpoint is taken in the homogenization theory for random heterogeneous and composite materials (see, e.g., [22, 30]). However, for the study of rare material failure events, standard homogenization theory is not enough to capture rare events, despite the recent advances in the understanding of variance scaling and the central limit theorem [3, 12, 13, 24]. Here our focus is on developing efficient numerical methods for the computation of the material failure probability via importance sampling.

We consider the material failure criterion such that under the external force, the strain of the elastic deformation exceeds a prefixed level at some point. More precisely, let $b \gg 1$ be the given threshold, the failure probability is defined as

$$(1.4) \quad P \left\{ \sup_{x \in D} |\nabla u| \geq b \right\}.$$

It is well known that to simulate such small probabilities is a difficult challenge for the direct Monte Carlo method. Instead, we employ importance sampling techniques for the computation of the failure probability.

In this paper, we propose an efficient Monte Carlo method via importance sampling to compute the small failure probabilities as in (1.4) when the differential equation is driven by a Gaussian random field as in (1.3). The change of measure proposed in this paper is not of the exponential tilting form and therefore is nonstandard. In the one-dimensional setting, the algorithm can be proved to be asymptotically efficient. For the case in higher dimensions, due to the lack of large deviations results,

efficiency cannot be rigorously established. However, the algorithm does admit a very good performance in our numerical studies.

There is a long history of study of material failure and structure safety in the civil engineering and material sciences from the probabilistic viewpoint or the extreme value theory. The important role of Weibull distribution [31] for the (idealized) weak-link principle is well established and applied in numerous engineering applications, although it faces lots of challenges for modeling real material properties. Making substantial progress toward this challenge is the well-known work of Bažant on the statistical size effect [4]. In contrast to these engineering statistical approaches for material/structure failures, we take the mechanistic approach by using the classical linear elasticity model, i.e., (1.1). It is admitted that many physical processes such as the development of fractures and cracks as well as dynamical failure scenarios are not shown in this model. Yet, it is a good prototype model, in the balance of tractability and complexity of modeling material failures. Nevertheless, probabilistic study of this model for high excursion of strain field is helpful to shed light on the extreme mechanical behaviors of random elastic media. Furthermore, our model is quite general and is never limited to the application of elastic mechanics. There are lots of other important physical and engineering problems modeled in exactly the same form as our elliptic equation (1.1) with random coefficients. For instance, the Darcy equation with uncertain coefficients is the canonical model for groundwater study where ∇u is an important physical quantity related to the phase speed of pollutants carried by groundwater.

In view of extremely small failure probabilities of concern here, our work fits into the general scope of works devoted to rare event simulations. Different approaches have been proposed in recent years for such problems, in particular in engineering and industrial applications. For instance, the idea of design point shift has been used in the framework of polynomial chaos expansion for failure events [27]. The numerical adaptive strategy is also tested on the PDE with random input data [26]. In terms of Monte Carlo importance sampling method which is free of the “curse of dimensionality,” the work [14] combines the cross-entropy method and the surrogate model to efficiently calculate the failure probabilities, which in principle works for very general problems. The recent work [28] applied the large deviation and importance sampling method to the calculation of the failure probability of hypersonic engines. We also mention the study of rare events in optical pulses modeled by the randomly perturbed one-dimensional nonlinear Schrödinger equation (see, e.g., [9, 23]). We refer to [10, 8, 2, 11] for general techniques of importance sampling and rare events simulations.

Our problem is also closely connected to the probabilistic theories for the Gaussian random field. For stochastic systems driven by light-tailed random variables (such as Gaussian random variables), it is customary to consider the exponential change of measure for the design of an efficient importance sampling algorithm. The parameters are usually selected by the minimal cross-entropy method [29] or some control problems related to the large deviation principle [10]. For heavy-tailed stochastic systems, some recent works are [7, 5, 6]. In the context of Gaussian processes and random fields, the most well-studied events are the high-level excursions (tail events of the supremum) [1]; the tail events of other convex functionals of Gaussian random fields are also of interest [18, 15, 16, 17]. The method in this paper is in part built on the results in this literature.

The rest of the paper is organized as follows. The description of the algorithm is given in section 2. Implementation details and numerical results are discussed in section 3. Conclusions and discussions are summarized in section 4.

2. The main method.

2.1. Rare event simulation, variance reduction, and importance sampling. Let us consider the problem of estimating a small probability $w = P(B) \ll 1$ or a family of probabilities $w(b) = P(B_b)$, where b is the rarity parameter that indicates the difficulty of the problem. In our case, we identify the rarity parameter as the threshold, and the event is given by $B_b = \{\sup_D |\nabla u| \geq b\}$. As b tends to infinity, the probability of interest $w(b) = P(B_b)$ tends to 0.

As the probabilities to be estimated are very small, the computational error needs to be quantified relative to the probabilities of interest. Let us consider an unbiased Monte Carlo estimator Z_b for $w(b)$ such that $\mathbb{E}Z_b = w(b)$. The (squared) relative error is given by $\text{Var}(Z_b)/w^2(b)$ or $\mathbb{E}(Z_b^2)/w^2(b) = 1 + \text{Var}(Z_b)/w^2(b)$. Suppose that n independent and identically distributed replicates of Z_b are generated, denoted by $Z_b^{(1)}, \dots, Z_b^{(n)}$. Let

$$\bar{Z}_n \triangleq \frac{1}{n} \sum_{i=1}^n Z_b^{(i)}$$

be the averaged estimator, whose variance is

$$\text{Var}(\bar{Z}_n) = \frac{\text{Var}(Z_b)}{n}.$$

Via Chebyshev's inequality, we obtain that

$$P(|\bar{Z}_n - w(b)| > \varepsilon w(b)) \leq \frac{\text{Var}(Z_b)}{n\varepsilon^2 w^2(b)}.$$

For any $\delta > 0$ if we intend to estimate $w(b)$ with at most ε relative error with at least probability $1 - \delta$, then it suffices to generate

$$n = \frac{\text{Var}(Z_b)}{w^2(b)} \delta^{-1} \varepsilon^{-2}$$

samples. Hence, the necessary sample size is proportional to the relative error $\text{Var}(Z_b)/w^2(b)$.

Consider the direct Monte Carlo estimator I_{B_b} . Its relative error is

$$\frac{\text{Var}(I_{B_b})}{w^2(b)} = \frac{1 - w(b)}{w(b)} \rightarrow \infty$$

as $w(b) \rightarrow 0$. The necessary sample size is $n = w^{-1}(b)\delta^{-1}\varepsilon^{-2}$ and I_{B_b} is considered an inefficient estimator for $w(b)$ when $w(b)$ is very small. There are several efficiency criteria in the literature [8, 2]. The most widely used is *weak efficiency*, or *asymptotic efficiency*, requiring that for all $\epsilon > 0$, $\mathbb{E}(I_{B_b}^2)/w^2(b) = o(w^{-\epsilon}(b))$ as $w(b) \rightarrow 0$. In the numerical analysis, we will investigate the relative errors of the proposed estimator. The empirical study shows that our estimator admits reasonably small relative errors (less than 10) when $w(b)$ is very small (less than 10^{-6}), although rigorous efficiency is difficult to establish and is beyond the scope of this paper.

In the subsequent analysis, we employ importance sampling as the main variance reduction technique that is based on the following identity:

$$P(B) = \int I(\omega \in B)P(d\omega) = \int I(\omega \in B)\frac{dP}{dQ}Q(d\omega) \quad \text{for all measurable set } B$$

for a measure Q such that $Q(\cdot \cap B)$ is absolutely continuous with respect to the measure $P(\cdot \cap B)$. As a consequence, we have that

$$Z(\omega) = I(\omega \in B) \frac{dP}{dQ}(\omega)$$

is an unbiased estimator of $P(B)$ under Q . In other words, $\mathbb{E}^Q Z = P(B)$, where \mathbb{E}^Q is the expectation with respect to the measure Q ,

It is easy to verify that if we choose $\mathcal{Q} = P(\cdot|B) = P(\cdot \cap B)/P(B)$, then the corresponding importance sampling estimator admits zero variance. Thus, we often call \mathcal{Q} the zero-variance change of measure. On the other hand, \mathcal{Q} is clearly of no practical value, in that the likelihood ratio is almost surely $P(B)$, which is precisely the quantity we want to compute. Nevertheless, the measure \mathcal{Q} provides a guideline to construct a change of measure for the efficient computation of $P(B)$. We need to construct a measure Q that is close to \mathcal{Q} such that we are capable of sampling from Q and computing the Radon–Nikodym derivative dQ/dP to achieve variance reduction.

2.2. The change of measure. Let us characterize a measure Q for the random field ξ as in (1.3) defined on the continuous sample path space $\mathcal{C}(D)$, where $\xi : D \rightarrow \mathbb{R}$ is a realization of the random field and D is the domain of the PDE. Our choice of Q depends on two probability density functions $h(\cdot)$ and $g_x(\cdot)$ to be determined later. Given h and g , the Radon–Nikodym derivative of Q with respect to P is given by

$$(2.1) \quad \frac{dQ}{dP}(\xi) = \int_D h(x) \frac{g_x(\xi(x))}{\phi_x(\xi(x))} dx.$$

Here, for each point $x \in D$, $\phi_x(\cdot)$ is the marginal density function of $\xi(x)$ under P , that is,

$$\int_A \phi_x(y) dy = P(\xi(x) \in A) \quad \text{for any measurable set } A \subset \mathbb{R}.$$

In (2.1), $h(\cdot)$ is a density function over the domain D and $g_x(\cdot)$ for each $x \in D$ is a density function on \mathbb{R} . We will choose h and g_x such that the corresponding measure Q is a good approximation of \mathcal{Q} for variance reduction.

Let us first explain how to sample from Q before discussing the choices of h and g_x . It consists of three steps.

ALGORITHM 2.1.

1. *Sample a random index (position) $x \in D$ following the density $h(x)$;*
2. *Conditional on the realized x , sample a random number $\xi(x)$ following the density $g_x(\cdot)$;*
3. *Conditional on the realized x and $\xi(x)$, sample ξ on $D \setminus \{x\}$ from the conditional distribution $P\{\xi \in \cdot \mid \xi(x)\}$.*

It is easy to verify that the above three-step procedure is consistent with the Radon–Nikodym derivative (2.1). Let $Q(\xi)$ be the probability of ξ under Q . Noticing that the third step in Algorithm 1 is done actually under P , we have

$$\begin{aligned} Q(\xi) &= \int_D \int_{\mathbb{R}} dx d\alpha h(x) g_x(\alpha) P(\xi(x') : x' \in D \setminus \{x\} \mid \xi(x) = \alpha) \\ &= \int_D \int_{\mathbb{R}} dx d\alpha h(x) \frac{g_x(\alpha)}{\phi_x(\alpha)} P(\xi(x) = \alpha) P(\xi(x') : x' \in D \setminus \{x\} \mid \xi(x) = \alpha) \end{aligned}$$

$$\begin{aligned}
&= \int_D \int_{\mathbb{R}} dx d\alpha h(x) \frac{g_x(\alpha)}{\phi_x(\alpha)} P(\xi(x') : x' \in D \setminus \{x\} \text{ and } \xi(x) = \alpha) \\
&= \int_D dx h(x) \frac{g_x(\xi(x))}{\phi_x(\xi(x))} P(\xi),
\end{aligned}$$

which validates (2.1) by noting $P(\xi)$ is independent of the x variable. If $g_x = \phi_x$ for all $x \in D$, then we have $Q = P$. In addition, the above derivation shows that the distributions of ξ under P and Q are different only at one random location that is labeled by x , whose distribution is given by h . This suggests that if the occurrence of the rare event $\{\sup_{x \in D} |\nabla u(x)| > b\}$ is mostly due to the abnormal behavior of the random field ξ at one location, our Q would be a good candidate of approximating the zero-variance change of measure \mathcal{Q} . In this sense, the distribution of the random index x (i.e., $h(x)$) should be approximately the distribution of the location where ξ deviates mostly from its original law under P , *conditioned* on the occurrence of material failure. Furthermore, the distribution g_x characterizes how $\xi(x)$ deviates from its original law ϕ_x . In what follows, we will describe in detail the choices of g_x and h .

2.3. The excursion level and the choice of g_x . Bearing in mind the above intuition, we proceed to describing h and g_x . Among these two, g_x is more important as it quantifies the deviation of ξ from its original law. The basic idea is as follows. If $\sup_D |\nabla u(x)|$ admits an excursion over some high level b , then the process $\sup_D \xi(x)$ must also have a high excursion over some level l_x depending on b and the precise location x where the excursion occurs. This observation is due to the connection between ξ and u in the PDE (1.1). Therefore, we expect that, in our important sampling scheme, $\xi(x)$ must reach the high level l_x quite easily under the distribution g_x . One apparent choice of such a distribution for g_x is a Gaussian distribution whose mean is specified as l_x , although we do not exclude other possibilities like student distribution with a similar shifted mean determined by l_x .

In the analysis of the one-dimensional equation, an explicit formula is available for the solution to the differential equation,

$$u'(x) = e^{\xi(x)} \left\{ -F(x) + \frac{\int_D F(x) e^{\xi(y)} dy}{\int_D e^{\xi(y)} dy} \right\},$$

where $F(x) = \int_0^x f(y) dy$. Notice that $F(x)$ is a bounded function and thus $\log u'(x) = \xi(x) + \mathcal{O}(1)$. Hence $\sup |u'(x)| > b$ implies $\sup |\xi(x)| > \log b + \mathcal{O}(1)$. Based on this closed form solution, it is reasonable to consider that l_x is approximately $\log b$. The optimal choice of l_x would be of order $\log b + \mathcal{O}(\log \log b)$. In the high-dimensional analysis, the PDE does not have a closed form solution. It is generally difficult to derive an analytic relationship between b and l_x . Nevertheless, we conjecture that the relationship $l_x \approx \log b$ is generally appropriate. This would be justified in our numerical examples.

Based on the above discussion, we choose l_x such that it is just enough for $\sup_D |\nabla u(x)|$ to exceed b . In particular, for each $x_0 \in D$ and l , we define

$$\xi_{l,x_0}(x) = lC(x - x_0) = E\{\xi(x) \mid \xi(x_0) = l\},$$

where $C(\cdot)$ is the covariance function of ξ , that is,

$$C(x) = \text{Cov}(\xi(y), \xi(y + x)).$$

The fact $lC(x - x_0) = E\{\xi(x) \mid \xi(x_0) = l\}$ is due to that $\xi(x)$ has zero mean and unit variance. For other cases, the form of conditional expectation can be adapted. Let $u_{l,x_0}(x)$ be the solution to the PDE (1.1) with $a(x) = e^{-\xi_{l,x_0}(x)}$. Then, l_{x_0} is given by

$$(2.2) \quad l_{x_0} = \min \left\{ l \in \mathbb{R} : \sup_{x \in D} |\nabla u_{l,x_0}(x)| \geq b \right\}.$$

We now provide an intuitive explanation for the above choice of l_x . The basic understanding is that the high excursion of $|\nabla u|$ is caused by the high excursion of the input process ξ . In order to determine the necessary excursion level, we perform the following calculations. Conditional on $\xi(x_0) = l_{x_0}$ that is a large number, the conditional field, denoted by $\tilde{\xi}$, has the following representation:

$$\tilde{\xi}(x) = l_{x_0}C(x - x_0) + r(x - x_0),$$

where $r(x)$ is a zero-mean Gaussian process whose covariance function can be obtained by conditional Gaussian calculations. The rationale of (2.2) is as follows. The process $r(x)$ is the remainder process after taking out the conditional mean and $r(x)$ is of a constant order. If l_{x_0} is selected to be large, then the variation of $r(x)$ is negligible compared to the conditional mean. Therefore, the conditional field can be approximated by

$$\tilde{\xi}(x) \approx l_{x_0}C(x - x_0).$$

By solving (2.2), l_{x_0} is the minimum level that $\xi(x)$ needs to achieve conditioned on that $\sup |\nabla u(x)|$ just exceeds b .

Having l_x defined, we then choose g_x to be the Gaussian distribution

$$(2.3) \quad g_x \sim \mathcal{N}(l_x, l_x^{-2}).$$

The choice of the variance of g_x aims at approximating the conditional variance of $\xi(x)$ under P with the condition that $\xi(x) > l_x$, where l_x is a large number. Notice that $\xi(x)$ is a standard Gaussian random variable for any fixed x under P . Following the fact that conditional on $\xi(x) > l_x$, $\xi(x) - l_x$ is asymptotically an exponential random variable with variance $\sim l_x^{-2}$, the variance in g_x is thus also l_x^{-2} to match the scale of the variance. In the simulation study, we also vary the choices of this variance and find that l_x^{-2} yields the best numerical results in terms of variance reduction. For each $x_0 \in D$, we provide an iterative algorithm to compute l_{x_0} .

ALGORITHM 2.2. Initialize $l_{x_0}^{(0)} = \log b$ and $n = 0$

while “not converge” **do**

- 1. Solve the PDE (1.1) for $\xi(x) = l_{x_0}^{(n)}C(x - x_0)$ numerically. Denote the solution by $u^{(n)}$.
- 2. Set $l_{x_0}^{(n+1)} = l_{x_0}^{(n)} - \log \sup |\nabla u^{(n)}| + \log b$.

When converged, the above algorithm yields a level $l_{x_0}^{(\infty)}$ satisfying (2.2). Furthermore, if $\xi(x) = l_{x_0}C(x - x_0)$, then we expect that $\sup_D |\nabla u|$ and l_{x_0} have the following relationship:

$$(2.4) \quad \sup_D |\nabla u| \sim \kappa_{x_0} l_{x_0}^\alpha e^{l_{x_0}}.$$

This relationship is correct for the one-dimensional case and is conjectured for the high-dimensional case (we will verify this numerically in section 3). Assuming (2.4), Algorithm 2.2 is asymptotically the Newton–Raphson algorithm for the equation

$$\kappa_{x_0} l_{x_0}^\alpha e^{l_{x_0}} = b.$$

Given the initial value $l_{x_0}^{(0)} = \log b$, it can be shown that $|l_{x_0}^{(2)} - l_{x_0}^{(\infty)}| = o(1/\log b)$, which is accurate enough for the construction of an efficient importance sampling. Therefore, in our implementation, we take only very few iterations in Algorithm 2.2.

2.4. The choice of h . We now proceed to the other tuning parameter, the distribution h . Let the notation x represent the location of the largest deviation from the original distribution. Such a deviation is quantified by the level l_x for each x . For each $x \in D$, we then choose

$$h(x) \propto P\left\{\xi(x) > l_x \mid \sup_D |\nabla u| > b\right\} \propto P\{\xi(x) > l_x\}.$$

The second \propto is true because the event $\sup_D |\nabla u| > b$ does not explicitly depend on x or l_x at all. After normalization, we get

$$(2.5) \quad h(x) = \frac{P(\xi(x) > l_x)}{\int_{y \in D} P(\xi(y) > l_y) dy}.$$

Sampling from h requires the numerical evaluation of l_x which induces some computational overhead. To further reduce the computational complexity, we will evaluate l_x for a finite grid that spreads over the domain D and use an interpolation for the rest of the domain. Details will be presented in the subsequent section.

2.5. Summary. Based on the above description, we generate the process $\xi(x)$ according to Algorithm 2.1. The tuning distributions g_x and h are given in (2.3) and (2.5), where l_x is defined through (2.2). Finally the importance sampling estimator is

$$Z_b = I(\sup |\nabla u(x)| > b) \left(\int_D h(x) \frac{g_x(\xi(x))}{\phi_x(\xi(x))} dx \right)^{-1}.$$

For the implementation, we discretize the space, the details of which are presented in the following section.

Remark. If the stationary Gaussian random field ξ is not standard, i.e., the mean $E\xi = \mu$ and the variance $\text{Var} \xi = \sigma^2$, the above calculations need the following slight modification after transforming ξ to the standard version $\bar{\xi}$. Write $\xi(x) = \sigma(\bar{\xi}(x) - \mu)$ and let $\bar{C}(x)$ be the covariance function for the standard process $\bar{\xi}$. Then the excursion function for $\bar{\xi}$, denoted by \bar{l}_{x_0} , has the same form as (2.2) except that the solution u_{l, x_0} now is associated to the stiffness parameter in the form of $a(x) = \exp(-\sigma(l\bar{C}(x-x_0) - \mu))$. The formulas (2.3) and (2.5) are still valid after using the “bar” version: \bar{l}_x and $\bar{\xi}$. During the importance sampling procedure, the standard $\bar{\xi}$ is first sampled from the Q associated with (2.3) and (2.5), and then $a(x) = \exp(-\sigma(\bar{\xi}(x) - \mu))$ is used to solve the PDE. The likelihood ratio (2.1) is still valid with the new defined g_x and h .

3. Numerical details and examples. We will present numerical examples for one-dimensional and two-dimensional cases. The domain for the one-dimensional PDE is $[0, 1]$ and the domain for the two-dimensional PDE is $D = [0, 1] \times [0, 1]$. The covariance function of the Gaussian field ξ in both cases is

$$(3.1) \quad E\{\xi(x)\xi(y)\} = C(x-y) = \exp(-|x-y|^2/R^2),$$

where $|\cdot|$ is the Euclidean distance. The scalar R is known as the correlation length of the random field. The boundary condition is Dirichlet $u|_{\partial D} = 0$ unless specified otherwise. Our numerical results consist of a verification of the exponential relationship between $\max \xi(x)$ and $\max |\nabla u(x)|$, visualization of the excursion level l_x , and empirical performances of the importance sampling algorithm in estimating the failure probabilities.

3.1. Implementation of the algorithm. To sample the random field ξ , we first need to discretize the domain D and use the field on the discrete mesh grid as an approximation. Denote a point in \mathbb{R}^2 as $x = (x^1, x^2)$. Choose a discrete mesh $\widehat{D}_N \triangleq \{(x_i^1, x_j^2)\}$, where $0 = x_0^1 < x_1^1 < \dots < x_{n_1}^1 = 1$, $0 = x_0^2 < x_1^2 < \dots < x_{n_2}^2 = 1$ and $n_1 \times n_2 = N$. Then any sample path of the continuous random field $\xi(x)$ is approximated by the N -dimensional random vector $(\xi(x_i^1, x_j^2) : 1 \leq i \leq n_1, 1 \leq j \leq n_2)$. The following is the discrete analogue of Algorithm 2.1 on the grid.

ALGORITHM 3.1.

1. Sample a random index $\tau \in \widehat{D}_N$ following the weight $h(\tau)\delta_\tau$ as in (2.5), where δ_τ is the corresponding Lebesgue measure of the cell associated to τ in the mesh \widehat{D}_N .
2. Conditional on the realized τ , sample $\xi(\tau)$ following the density $g_\tau(\cdot) \sim N(l_\tau, l_\tau^{-2})$;
3. Conditional on the realized τ and $\xi(\tau)$, sample $\{\xi(x) : x \in \widehat{D}_N\}$ from the conditional distribution $P(\xi \in \cdot | \xi(\tau))$;
4. Solve PDE (1.1) with $a(x) = \exp(-\xi(x))$ and calculate $\sup_{x \in D} |\nabla u(x)|$;
5. Output the estimator

$$Z_b = I(\sup_D |\nabla u(x)| > b) \left[\sum_{x \in \widehat{D}_N} h(x)\delta_x \cdot \frac{g_x(\xi(x))}{\phi_x(\xi(x))} \right]^{-1}.$$

We now provide further details on steps 3 and 4 in the above algorithm. Step 3 generates a random vector ξ on \widehat{D}_N given a realization $\xi(\tau)$. Notice that ξ on \widehat{D}_N is a multivariate Gaussian random vector and thus the conditional distribution is still multivariate Gaussian. The conditional mean is $\mathbb{E}\{\xi(x) | \xi(\tau) = y\} = y \times C(x - \tau)$ and the conditional covariance matrix is $\widehat{C}_{N-1, N-1} - \widehat{C}_{N-1, 1} \widehat{C}_{N-1, 1}^T$. Here, \widehat{C}_N is the N by N unconditional covariance matrix, $\widehat{C}_{N-1, 1}$ is column of \widehat{C}_N corresponding to τ with row corresponding to τ deleted, and $\widehat{C}_{N-1, N-1}$ is hence the $(N-1) \times (N-1)$ submatrix of \widehat{C}_N with row and column corresponding to τ deleted. However, in generating this conditional sample, we do not need to decompose the conditional covariance matrix. A simple procedure $\xi(x) \triangleq \xi'(x) + \widehat{C}(x - \tau)(\xi(\tau) - \xi'(\tau))$ for all $x \in \widehat{D}_N$ gives the conditional sample $\{\xi(x) : x \in \widehat{D}_N\}$ with the known (conditional) value of $\xi(\tau)$, where $\{\xi'(x) : x \in \widehat{D}_N\}$ is the N -dim Gaussian vector with covariance matrix \widehat{C}_N . To sample the multivariate Gaussian random vectors $\{\xi'(x) : x \in \widehat{D}_N\}$, we adopt the Cholesky decomposition of the covariance matrix that is computed via the pivoted Cholesky factorization [21] in LAPACK 3.2. Due to stationarity, this decomposition needs to be computed only once.

Once a realization of ξ is generated, the PDE (1.1) is solved by a standard numerical solver. Many traditional advanced numerical strategies such as adaptive mesh refinement could be used to improve the efficiency and the accuracy of the PDE solver. For the numerical examples in this paper, we use the finite volume method on a uniform mesh in D . This simple strategy is adequate in our work to demonstrate the performance of the variance reduction with a sufficiently high resolution of the mesh grid.

In summary, our preprocessing includes a Cholesky factorization of the covariance matrix and solving an inverse problem to obtain the excursion level function l_x . In what follows, we present various numerical results related to our rare event calculation of the failure probabilities.

3.2. Verification of exponential relationship. We start from a numerical verification of our conjecture about the maximums of ξ and $|\nabla u|$. Our algorithm and analysis depend on the following scaling relationship between the input field ξ and the strain field ∇u , whenever either of them has a high excursion,

$$(3.2) \quad \sup_D \xi \sim \sup_D \log |\nabla u|,$$

which is to be verified in this subsection.

In the one-dimensional case, the explicit formula of u and ∇u renders the verification of the above relation quite obvious for any bounded external force. For the problem of higher dimension, as explicit solution is not available, the rigorous justification of (3.2) is more challenging. Here, we numerically verify this relationship via a stochastic approach and a deterministic approach. In the stochastic approach, one spatial location $x^* \in D$ is selected and a sequence of the excursion levels l is selected. For each l , we generate a random sample path $\xi(x)$ conditioned on $\xi(x^*) = l$. We then calculate the maximum value of the strain $\max |\nabla u|$ corresponding to the generated $\xi(x)$ and we set the homogeneous force $f(x) \equiv 1$. In the left panel of Figure 1, we plot $\log(\max |\nabla u|)$ versus $\max \xi$ for different spatial locations x^* . For the deterministic approach, we observe that for l sufficiently large, the conditional field is approximately $\xi(x) \approx lC(x - x^*)$, as discussed in section 2. Hence, we solve the PDE with simply setting $\xi = lC(x - y)$, where C is the covariance function (3.1). The numerical results are in the right panel of Figure 1.

The numerical results in Figure 1 confirm that $\max \log |\nabla u|$ is asymptotically linearly proportional to $\max \xi$ and thus justify (3.2). When the external force f is inhomogeneous, a similar relationship can be established numerically. Furthermore, when comparing the results for different correlation lengths, we found that smaller correlation length yields lower $\max |\nabla u|$. Thus, for smaller correlation length, to ensure that $\max |\nabla u|$ reaches a level b , the larger values of $\max \xi$ are required, consequently suggesting a higher excursion level function l_x .

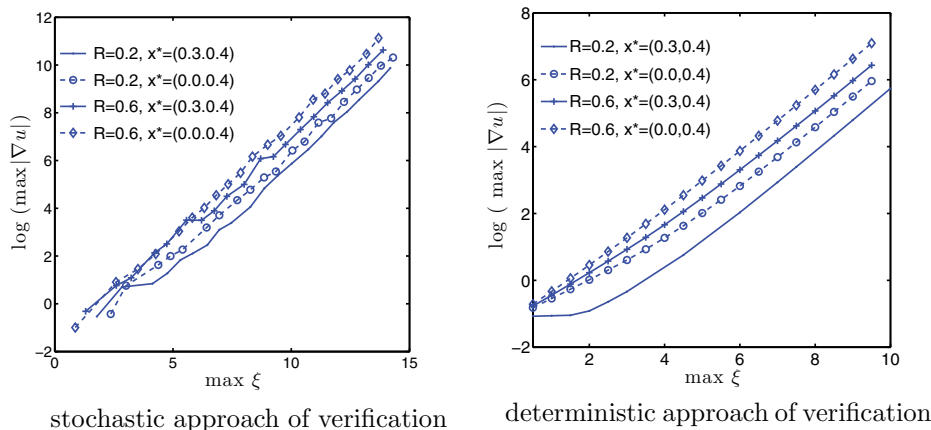


FIG. 1. Numerical verification of $\max |\nabla u| \sim \exp(\max(\xi))$. The domain is $D = [0, 1]^2$. The left panel is the stochastic approach where for each different value of l , one sample path of $\xi(x)$ is generated conditional on $\xi(x^*) = l$. Due to the randomness, l is not exactly equal to, but very close to, the sampled maximum $\max \xi$. The right panel is the deterministic approach where $\xi(x) = lC(x - x^*)$ is deterministic and l is precisely the maximum of ξ .

3.3. Excursion level function l_x . The excursion level function l_x characterizes the spatial distribution of the extreme values of $\xi(x)$ conditional on the failure event. We have explained how to find this function in section 2.3. The density function h is determined by l_x via (2.5) and the smaller value of l_x implies a higher likelihood of observing an excursion at or around x .

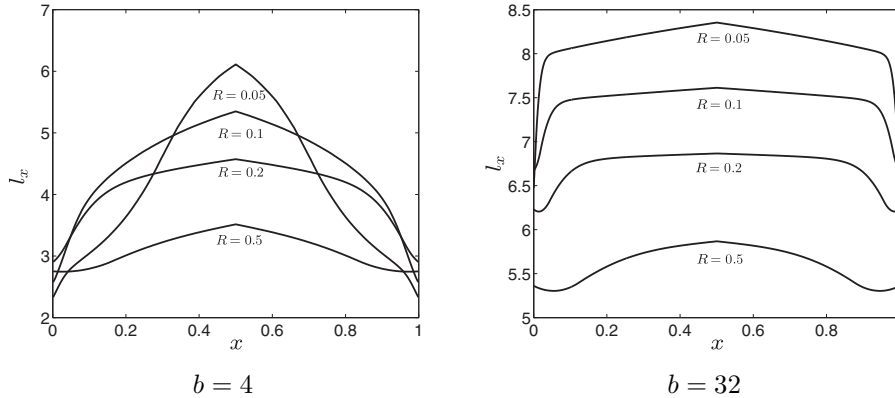


FIG. 2. The excursion level functions l_x corresponding to $b = 4$ and $b = 32$ for different correlation lengths R . $f \equiv 1$.

We now explore the function l_x for different external force functions f . Figure 2 shows the excursion level functions for the one-dimensional problem with $D = [0, 1]$ and f is set to be a constant. Due to the Dirichlet boundary condition, the excursion level function l_x is not a constant and it has significantly lower values close to the boundary, especially when the correlation length R is small. Thus, ξ has a higher probability to exhibit high excursions near the boundary than inside the domain, so it is for ∇u . The calculation of l_x for the two-dimensional case also confirms this boundary effect. Refer to Figure 3 for the two choices of external force. In Figure 3, left, the external force is homogeneous $f(x) \equiv 1$. In Figure 3, right, the external force has a discontinuity at $x_1 = 0.5$:

$$f(x) = \begin{cases} 1 & \text{if } x_1 \leq 0.5. \\ -1 & \text{if } x_1 > 0.5. \end{cases}$$

The local dip of the excursion level function l_x near this discontinuity is consistent with the physical heuristics that the material is easy to break down at this discontinuity line.

The dependence of the excursion level function on the correlation length R is suggested in Figure 2 from which smaller R requires larger l_x . However, it should be noted that this does not imply a smaller failure probability for smaller R , because it is easier for a Gaussian random function with smaller R to generate high excursions.

We checked the effectiveness of the obtained excursion level function for the importance sampling scheme by investigating the conditional sample of ξ given that the failure event $\sup |\nabla u| > b$ occurs. Using direct Monte Carlo for a moderate b with f being constant, we generated a few samples (not a large amount) given the failure events. We observed a common feature of their spatial profiles from these samples: there admits a unique and very high global maximum for each sample of ξ near the

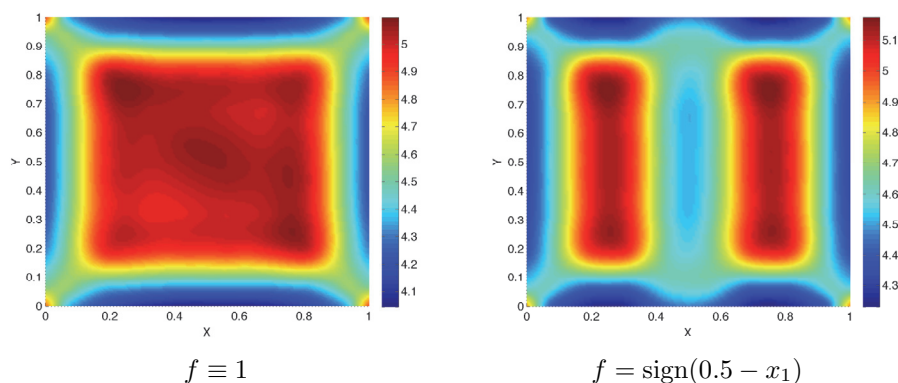


FIG. 3. Contour plot of the excursion level function l_x for reaching $\max |\nabla u| > b$ with homogeneous external force $f \equiv 1$ (left panel) and the discontinuous external force $f = \text{sign}(0.5 - x_1)$ (right panel). The correlation length is $R = 0.2$. The threshold is $b = 4$.

boundary, where the excursion level function l_x has dips. It is worth mentioning that there are several *local* maxima in the domain, but these local maxima are significantly lower than the global one. Most of the strain fields $|\nabla u|$ corresponding to these samples of ξ show a global maximum close to the global maximizer of ξ .

3.4. On the computation of the failure probabilities. Table 1 summarizes the performance of direct Monte Carlo method (MC) and the proposed importance sampling method (IS) described in Algorithm 3.1 for the failure probabilities for the one-dimensional differential equation. Table 2 shows the results for the two-dimensional case with two resolutions of grid mesh, 25×25 and 50×50 . In these tables, “ \hat{p}_b ” columns are the estimated probabilities. The “std” columns include the standard deviation per sample. The “rel. err.” is the ratio of std over \hat{p}_b . For very large values of b , e.g., $b = 16$ or 32 , the direct Monte Carlo fails to yield reasonable estimates as the failure event has not been observed in the finite number of samples. In this case, \hat{p}_b and std are marked as “-” but the relative error, rel. err., is calculated by the theoretic result $\sqrt{1/p} - 1$ with p being the estimated \hat{p}_b from the importance sampling method.

The relative error measures the relative efficiency of the Monte Carlo schemes. The comparison of relative errors in the last columns of Tables 1 and 2 shows that for all values of the threshold b , the proposed importance sampling scheme substantially outperforms the direct Monte Carlo method. When the event becomes rarer, its

TABLE 1

The estimated failure probabilities $P(\max |\nabla u| > b)$ for the one-dimensional equation where $f \equiv 1$, $R = 0.1$, and $N = 400$ based on 10^6 independent Monte Carlo samples in both direct Monte Carlo and the importance sampling. Asterisks indicate that relative error is given by $\sqrt{p^{-1}} - 1$, where p is estimated from our proposed method.

| b | \hat{p}_b | | std | | rel. err. | |
|-----|-------------|---------|---------|---------|-----------|------|
| | MC | IS | MC | IS | MC | IS |
| 2 | 2.15e-1 | 2.15e-1 | 4.12e-1 | 5.33e-1 | 1.91 | 2.48 |
| 4 | 3.06e-2 | 3.02e-2 | 1.74e-1 | 7.78e-2 | 5.63 | 2.54 |
| 8 | 2.75e-4 | 3.47e-4 | 1.66e-2 | 8.29e-4 | 60.4 | 2.39 |
| 16 | - | 1.08e-5 | - | 2.90e-5 | 302* | 2.69 |
| 32 | - | 1.89e-7 | - | 5.61e-7 | 2300* | 2.97 |

TABLE 2

The estimated failure probabilities $P(\max|\nabla u| > b)$ for the two-dimensional equation, where $R = 0.6$ and $f \equiv 1$. Sample size is 10^6 .

| Mesh size 25×25 | | | | | | |
|--------------------------|-----------------|---------|---------|---------|-----------|------|
| b | \widehat{p}_b | | std | | rel. err. | |
| | MC | IS | MC | IS | MC | IS |
| 1 | 2.70e-1 | 2.69e-1 | 4.44e-1 | 2.53e-1 | 1.65 | 0.94 |
| 2 | 5.79e-2 | 5.78e-2 | 2.34e-1 | 6.16e-2 | 4.03 | 1.07 |
| 4 | 6.25e-3 | 6.27e-3 | 7.88e-2 | 7.53e-3 | 12.6 | 1.20 |
| 8 | 3.52e-4 | 3.57e-4 | 1.88e-2 | 5.07e-4 | 53.3 | 1.42 |
| 16 | 8.00e-6 | 1.11e-5 | 2.83e-3 | 1.82e-5 | 353.0 | 1.64 |
| 32 | - | 1.96e-7 | - | 3.60e-7 | 2253* | 1.84 |

| Mesh size 50×50 | | | | | | |
|--------------------------|-----------------|---------|---------|---------|-----------|------|
| b | \widehat{p}_b | | std | | rel. err. | |
| | MC | IS | MC | IS | MC | IS |
| 1 | 2.97e-1 | 2.97e-1 | 4.57e-1 | 2.80e-1 | 1.54 | 0.94 |
| 2 | 6.71e-2 | 6.73e-2 | 2.50e-1 | 7.26e-2 | 3.73 | 1.08 |
| 4 | 7.75e-3 | 7.72e-3 | 8.77e-2 | 9.27e-3 | 11.3 | 1.20 |
| 8 | 4.48e-4 | 4.66e-4 | 2.12e-2 | 6.73e-4 | 47.2 | 1.44 |
| 16 | 1.80e-5 | 1.55e-5 | 4.24e-3 | 2.56e-5 | 236.0 | 1.64 |
| 32 | - | 2.93e-7 | - | 5.20e-7 | 1847* | 1.78 |

TABLE 3

The standard deviation of the importance sampling estimator for difference choices of the variance $\sigma_\tau^2 \equiv \sigma^2$ when conditionally sampling $\xi(\tau)$.

| b | $1/l_x$ | $\sigma = 0.02$ | $\sigma = 0.1$ | $\sigma = 0.2$ | $\sigma = 0.3$ | $\sigma = 0.5$ | $\sigma = 1$ | $\sigma = 5$ |
|-----|-------------|-----------------|----------------|----------------|----------------|----------------|--------------|--------------|
| 4 | 0.24 ~ 0.30 | 7.40e-1 | 8.67e-3 | 9.43e-3 | 7.36e-3 | 8.66e-3 | 1.21e-2 | 2.81e-2 |
| 32 | 0.16 ~ 0.18 | 1.65e-6 | 3.07e-7 | 2.85e-7 | 3.22e-7 | 4.05e-7 | 5.61e-7 | 1.40e-6 |

advantage becomes more significant. The importance sampling scheme maintains a very mild increment of the relative errors so that it still remains to be single digit even when the probability is as small as 10^{-7} . Results based on different mesh sizes in Table 2 shows a relative difference around 10%. This indicates that the spatial resolution is fine enough to get a reasonably accurate numerically obtained efficiency of the estimators.

In Algorithm 3.1, the alternative distribution $g_\tau(\cdot)$ of the random variable $\xi(\tau)$ is suggested to the Gaussian $\mathcal{N}(l_\tau, \sigma_\tau^2)$ and the variance of this Gaussian is set to be $\sigma_\tau \sim (l_\tau)^{-1}$. To justify this choice of the variance, we compare different constant values of $\sigma_x \equiv \sigma$ and present the effect of σ on the performance of the resulting importance sampling scheme. The comparison is presented in Table 3. The (one-sample) standard deviations of the resulting importance sampling scheme are for different σ values. In addition, the typical values of the reciprocal of the excursion level l_x ($x \in D$) are also calculated for comparison. As clearly seen from the results in the table, the optimal choice of σ_τ is indeed around the reciprocal of the excursion level, $\frac{1}{l_\tau}$.

For a smaller correlation length $R = 0.2$, we test the algorithm with constant external force f . As the correlation length of the random field is smaller, we use a finer mesh grid (150×150) to resolve. The results obtained are shown in Table 4, which further confirms the efficiency of the importance sampling scheme.

3.5. On the asymptotics of the failure probabilities. The importance sampling method can be applied to efficiently calculate quantities related to the failure event. A direct application is that we can numerically characterize the asymptotic

TABLE 4

Two dimensions. $P(\max |\nabla u| > b)$. Correlation length $R = 0.2$. Mesh size 150×150 . Sample size 10^6 . $f \equiv 1$.

| b | \hat{p}_b | | std | | rel. err. | |
|-----|-------------|---------|---------|---------|-----------|------|
| | MC | IS | MC | IS | MC | IS |
| 1 | 3.58e-1 | 3.58e-1 | 4.80e-1 | 4.60e-1 | 1.34 | 1.29 |
| 2 | 3.02e-2 | 2.96e-2 | 1.71e-2 | 1.67e-2 | 5.67 | 5.64 |
| 4 | 8.65e-4 | 8.61e-4 | 2.94e-2 | 5.81e-3 | 34.0 | 6.75 |
| 8 | 1.20e-5 | 1.44e-5 | 3.46e-3 | 6.28e-5 | 289 | 4.36 |
| 16 | - | 1.54e-7 | - | 6.73e-7 | 2548* | 4.37 |
| 32 | - | 1.06e-9 | - | 1.29e-8 | 30715* | 12.1 |

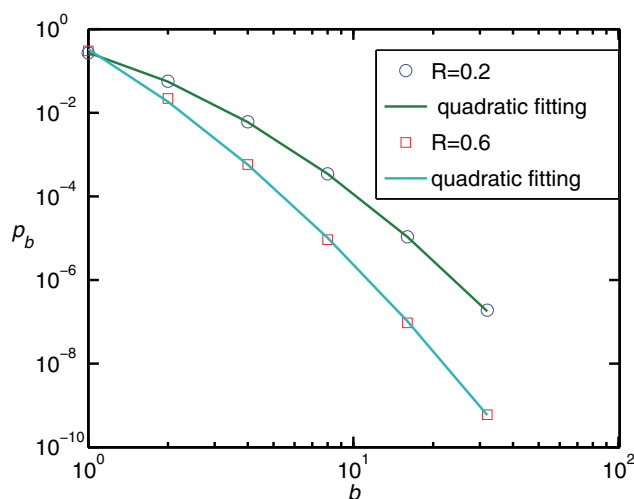


FIG. 4. \log - \log plot of p_b versus b from the data in Table 2, bottom, and Table 4. Set $\log p_b = q(\log b)$ and use the quadratic function for q for least square fitting. For $R = 0.6$, $q(x) = -0.65x^2 - 1.86x - 1.29$, and for $R = 0.2$, $q(x) = -0.59x^2 - 3.77x - 1.10$.

behavior of the tail probability $p_b = P(\sup_{x \in D} |\nabla u(x)| > b)$. For example, the data in the lower part of Table 2 and in Table 4 allow us to postulate an empirical asymptotics between $p_b = P(\max |\nabla u| > b)$ and b . Figure 4 shows the \log - \log plot of p_b versus b and the result of least square fitting. The result shows that the tail distribution satisfies

$$p_b = e^{q(\log b)},$$

where q is a quadratic function. Refer to Figure 4 for the specific expression for the examples calculated above. This quadratic dependency is consistent with our analytical result for the one-dimensional case [19, 20].

Figure 4 also shows an interesting result on the correlation length R . This figure and Tables 2 and 4 suggest that smaller correlation length leads to larger failure probability. This observation is consistent with the known effect for a Gaussian random field which has higher excursion probability for smaller correlation length. However, this result is not trivial here since here the excursion in failure event is for the random function $|\nabla u|$, which is apparently not Gaussian.

TABLE 5

One dimension. $P(\max |\nabla u| > b)$. Periodic boundary condition. $R = 0.2$. $Nx = 400$. Sample size 4×10^6 . $f = 10(x - 0.5)^2 - 5/6$.

| b | \hat{p}_b | | std | | rel. err. | |
|-----|-------------|---------|---------|---------|-----------|------|
| | MC | IS | MC | IS | MC | IS |
| 1 | 3.77e-2 | 3.76e-2 | 1.90e-1 | 2.28e-1 | 5.05 | 6.06 |
| 2 | 2.76e-3 | 2.40e-3 | 5.25e-2 | 8.80e-2 | 19.0 | 36.7 |
| 4 | 9.68e-5 | 7.17e-5 | 9.84e-3 | 3.22e-3 | 102 | 45.9 |
| 8 | 1.00e-6 | 1.51e-6 | 1.00e-3 | 1.82e-4 | 1000 | 121 |
| 12 | - | 1.28e-7 | - | 1.77e-5 | 2795* | 138 |

3.6. Numerical results under periodic boundary condition. We have demonstrated the efficiency of the variance reduction of our importance sampling scheme under the assumption of the Dirichlet boundary condition and the constant external force. Here, we test our method for the periodic boundary condition and nonhomogeneous body force. We only study a one-dimensional example where the domain of the elliptic equation is $D = [0, 1]$. To accommodate the periodic boundary condition, we first sample the values of the periodic random field $\xi(x)$ over the finite domain $[0, 1]$. This is done by simply designating a periodic covariance function $C_p(x)$. The function C_p is a period-1 extension of the original covariance function $C(x) = e^{-x^2/R^2}$, where $C_p(x) = C(x)$ for all $x \in [-1/2, 1/2]$. The solvability of the equation requires that $\int_0^1 f(x) = 0$. We consider the following quadratic function $f = 10(x - 1/2)^2 - 5/6$ in our example. The performance of the importance sampling scheme is shown in Table 5. The variance reduction is not as significant as the Dirichlet condition case but is still much better than the direct Monte Carlo for large b .

4. Conclusion and discussion. We present in this work an efficient importance sampling strategy for computing small probabilities associated with a materials failure problem modeled by a scalar elliptic equation with random log-normal coefficient. The change of measure used in the importance sampling is suggested by one-dimensional analysis and further justified numerically for higher dimensions. Our numerical results verify the superior behavior of the estimator over conventional approaches.

The asymptotic analysis of the failure probability, in particular, rigorously establishing the relation (3.2) is a very interesting open problem.

In this work, for simplicity, we have used the scalar model; however, there is no conceptual difficulty in generalizing our method to linear elastic models, which would be of interest for practical applications.

The efficient sampling technique for the failure event opens the door to many interesting applications. One particularly interesting application would be the design of materials in consideration of minimizing the failure probability. This gives rise to interesting future directions to explore.

REFERENCES

- [1] R. J. ADLER, J. H. BLANCHET, AND J. LIU, *Efficient Monte Carlo for large excursions of Gaussian random fields*, Ann. Appl. Probab., 22 (2012), pp. 1167–1214.
- [2] S. ASMUSSEN AND P. GLYNN, *Stochastic Simulation: Algorithms and Analysis*, Springer, New York, 2007.
- [3] G. BAL, *Central limits and homogenization in random media*, Multiscale Model. Simul., 7 (2008), pp. 677–702.
- [4] Z. P. BAŽANT, *Scaling theory for quasibrittle structural failure*, Proc. Natl. Acad. Sci. USA, 101 (2004), pp. 13400–13407.

- [5] J. H. BLANCHET AND J. LIU, *State-dependent importance sampling for regularly varying random walks*, Adv. Appl. Probab., 40 (2008), pp. 1104–1128.
- [6] J. H. BLANCHET AND J. LIU, *Efficient simulation and conditional functional limit theorems for ruinous heavy-tailed random walks*, Stoch. Proc. Appl., 122 (2012), pp. 2994–3031.
- [7] J. H. BLANCHET, P. GLYNN, AND J. C. LIU, *Fluid heuristics, Lyapunov bounds and efficient importance sampling for a heavy-tailed G/G/1 queue*, Queueing Syst., 57 (2007), pp. 99–113.
- [8] J. BUCKLEW, *Large Deviation Techniques in Decision, Simulation and Estimation*, Wiley, New York, 1990.
- [9] M. D. GRAHAM AND L. K. WILLIAM, *An iterative stochastic method for simulating large deviations and rare events*, SIAM J. Appl. Math., 71 (2011), pp. 903–924.
- [10] P. DUPUIS AND H. WANG, *Importance sampling, large deviations, and differential games*, Stoch. Stoch. Rep., 76 (2004), pp. 481–508.
- [11] W. E AND E. VANDEN-EIJNDEN, *Transition path theory and path-finding algorithms for the study of rare events*, Ann. Rev. Phys. Chem., 61 (2010), pp. 391–420.
- [12] A. GLORIA AND F. OTTO, *An optimal variance estimate in stochastic homogenization of discrete elliptic equations*, Ann. Probab., 39 (2011), pp. 779–856.
- [13] A. GLORIA AND F. OTTO, *Quantitative results on the corrector equation in stochastic homogenization*, preprint, arXiv:1409.0801, 2014.
- [14] J. LI, J. LI, AND D. XIU, *An efficient surrogate-based method for computing rare failure probability*, J. Comput. Phys., 230 (2011), pp. 8683–8697.
- [15] J. LIU, *Tail approximations of integrals of Gaussian random fields*, Ann. Probab., 40 (2012), pp. 1069–1104.
- [16] J. LIU AND G. XU, *Some asymptotic results of Gaussian random fields with varying mean functions and the associated processes*, Ann. Statist., 40 (2012), pp. 262–293.
- [17] J. LIU AND G. XU, *On the conditional distributions and the efficient simulations of exponential integrals of Gaussian random fields*, Ann. Appl. Probab., 24 (2014), pp. 1691–1738.
- [18] J. LIU AND G. XU, *On the density functions of integrals of Gaussian random fields*, Adv. in Appl. Probab., 45 (2013), pp. 398–424.
- [19] J. LIU AND X. ZHOU, *On the failure probability for one dimensional random material under delta external force*, Commun. Math. Sci., 11 (2013), pp. 499–521.
- [20] J. LIU AND X. ZHOU, *Extreme analysis of a random ordinary differential equation*, J. Appl. Probab., 51 (2014), pp. 1021–1036.
- [21] C. LUCAS, *LAPACK-Style Codes for Level 2 and 3 Pivoted Cholesky Factorizations*, LA-PACK Working Note 161, 2004.
- [22] G. MILTON, *The Theory of Composites*, Cambridge University Press, Cambridge, UK, 2002.
- [23] R. O. MOORE, G. BIONDINI, AND W. L. KATH, *A method to compute statistics of large, noise-induced perturbations of nonlinear Schrödinger solitons*, SIAM Rev., 50 (2008), pp. 523–549.
- [24] J. NOLEN, *Normal approximation for a random elliptic equation*, Probab. Theory Related Fields, 159 (2014), pp. 661–700.
- [25] M. OHRING, *Reliability and Failure of Electronic Materials and Devices*, Academic Press, New York, 1998.
- [26] P. CHEN AND A. QUARTERONI, *Accurate and efficient evaluation of failure probability for partial differential equations with random input data*, Comput. Methods Appl. Mech. Engrg., 267 (2013), pp. 233–260.
- [27] M. PAFFRATH AND U. WEVER, *Adapted polynomial chaos expansion for failure detection*, J. Comput. Phys., 226 (2007), pp. 263–281.
- [28] G. PAPANICOLAOU, N. WESTY, AND T.-W. YANG, *Probability of Failure in Hypersonic Engines Using Large Deviations*, arXiv:1208.5029, 2012.
- [29] R. Y. RUBINSTEIN AND D. P. KROESE, *The Cross-Entropy Method*, Springer, New York, 2004.
- [30] S. TORQUATO, *Random Heterogeneous Materials: Microstructure and Macroscopic Properties*, Springer, New York, 2001.
- [31] W. WEIBULL, *A statistical distribution function of wide applicability*, J. Appl. Mech., 18 (1951), pp. 293–297.